Available online at www.sciencedirect.com
ScienceDirect
Trans. Nonferrous Met. Soc. China 25(2015) 1027−1034
Transactions of Nonferrous Metals Society of China
www.tnmsc.cn

Effect of homogenization treatment on microstructure and mechanical properties of DC cast 7X50 aluminum alloy

Fu-guan CONG[1,2], Gang ZHAO[1], Feng JIANG[3], Ni TIAN[1], Rui-feng LI[1]

1. Key Laboratory for Anisotropy and Texture of Materials, Ministry of Education, Northeastern University, Shenyang 110004, China;
2. Northeast Light Alloy Co., Ltd., Harbin 150060, China;
3. School of Materials Science and Engineering, Central South University, Changsha 410083, China

Received 5 May 2014; accepted 20 October 2014

Abstract: The evolution of the eutectic structures in the as-cast and homogenized 7X50 aluminum alloys was studied by scanning electron microscopy (SEM), transmission electron microscopy (TEM), energy dispersive spectrometer (EDS), differential scanning calorimetry(DSC), X-ray diffraction(XRD) and tensile test. The results show that the main phases are $S(Al_2CuMg)$, $T(Al_2Mg_3Zn_3)$ and $MgZn_2$, with a small amount of Al_7Cu_2Fe and Al_3Zr in the as-cast 7X50 alloy. The volume fraction of the dendritic-network structure and residual phase decreases gradually during the homogenization. After homogenization at 470 °C for 24 h and then 482 °C for 12 h, the $T(Al_2Mg_3Zn_3)$ phase disappears and minimal $S(Al_2CuMg)$ phase remains, while almost no change has happened for Al_7Cu_2Fe. There is a strong endothermic peak at 477.8 °C in the DSC curve of as-cast alloy. A new endothermic peak appears at 487.5 °C for the sample homogenized at 470 °C for 1 h. However, this endothermic peak disappears after being homogenized at 482 °C for 24 h. The $T(Al_2Mg_3Zn_3)$ phase cannot be observed by XRD, which is consistent with that T phase is the associated one of $S(Al_2CuMg)$ phase and $MgZn_2$ phase. The volume fraction of recrystallized grains is substantially less in the plate with pre-homogenization treatment. The strength and fracture toughness of the plate with pre-homogenization treatment are about 15 MPa and 3.3 MPa·m$^{1/2}$ higher than those of the material with conventional homogenization treatment.

Key words: 7X50 aluminum alloy; microstructural evolution; homogenization; residual phase; recrystallization

1 Introduction

The mechanical properties of aluminum alloys depend largely on the alloying elements and their presence in the solid solution. During the solidification of aluminum alloys, a large portion of alloying elements may segregate into liquid and form coarse particles in the grain boundary (GB) regions or inside the grains. The chemical composition, casting and homogenization processes will influence the volume fraction, morphology, and intrinsic characteristics of these coarse particles [1−3]. These particles can deteriorate the hot workability especially when they are in the GB regions, and limit the range of applicable process parameters during subsequent hot deformation [4]. Usually, the residual coarse particles (>1 μm) such as Fe-rich or Cu-rich phases will deteriorate the toughness and fatigue properties [1,4−8]. The microstructures of the as-cast and homogenized Al−Zn−Mg−Cu alloys have been studied in recent years. Most of the investigations are focused on the nature, evolution and distribution of $Al_2Mg_3Zn_3$ (T), Al_2CuMg (S), $MgZn_2$ (η), $(AlCuZn)_2Mg$, Al_2Cu (θ), Al_7Cu_2Fe and $Al_{13}Fe_4$ phases during homogenization [9−21]. ZHAO et al [21] and RANGANATHA et al [22] studied the effects of homogenization treatment on the microstructural changes of AA7075 and 7049 alloys. LIM et al [23] studied the effects of constitutional changes and preheating conditions on the evolution of constituent particles, the M, T, and S phases, and dispersoids in AA7175 and AA7050 alloys. LI and STARINK [9] and FAN et al [10] studied the evolution of microstructure in an Al−Zn−Mg−Cu alloy during homogenization. LÜ et al [11] and MONDAL and MUKHOPADHYAY [20] studied the phases in the as-cast and homogenized 7055 aluminum alloy, and revealed that the major residual phases were $\eta(MgZn_2)$, $T(Al_2Mg_3Zn_3)$, $S(Al_2CuMg)$ and $\theta(Al_2Cu)$. The

Foundation item: Project (2011KJZX1-2) supported by the Science and Technology Development Fund of Aluminum Corporation of China
Corresponding author: Fu-guan CONG; Tel: +86-451-86564564; E-mail: cfgdy2010@163.com
DOI: 10.1016/S1003-6326(15)63694-9

microstructure of the as-cast 7050 alloy consists of dendrites, high angle grain boundaries, and inter-dendritic eutectic regions containing phases such as Al_2CuMg, $MgZn_2$ and Mg_2Si [14,15]. ROKHLIN et al [16] and LI and STARINK [17] studied the effects of Zr, Sc and Cr on microstructures and intermetallic phases in Al−Zn−Mg−Cu aluminium alloys.

Although some researches have been reported on the microstructure in as-cast condition and the evolution of the eutectic phases during homogenization in the case of Al−Zn−Mg−Cu series alloys, the information on the 7X50 aluminum alloys is still rarely seen in literature. Moreover, there is no comparative study on homogenized microstructure. The objectives of this work were to determine the effect of homogenization treatment on the microstructural evolution. The transformation from eutectic structures to coarse particles was also investigated.

2 Experimental

Cubic samples with dimensions of 20 mm × 20 mm × 20 mm were cut from the center of a semi-continuous casting AA7X50 ingot with the dimensions of 520 mm × 1600 mm. The chemical composition of this alloy is shown in Table 1. Single-stage homogenization treatment was performed at 470 °C for 1, 8, 24, 72, and 240 h, respectively. Double-stage homogenization treatment was performed at 470 °C for 24 h and then at 482 °C for 1, 2, 6, 24, and 72 h, respectively. Pre-homogenization treatment was performed at 400 °C for 10 h and then at 470 °C for 24 h. The homogenized samples were machined with dimensions of 100 mm × 250 mm × 300 mm. The blocks were rolled with seven passes up to 30 mm in thickness after being reheated at 380 °C for 4 h. Solution treatment of hot-rolled plates was carried out at 480 °C for 1 h and the samples were quenched immediately in water.

Table 1 Chemical composition of 7X50 aluminium alloy (mass fraction, %)

Zn	Mg	Cu	Zr	Fe	Si
6.43	2.32	2.08	0.10	0.08	0.05
Ti	Mn	Cr	Ni	Al	
0.03	<0.05	<0.04	<0.02	Bal.	

The microstructures of different homogenized samples etched using Keller's etchant (2 mL HF + 3 mL HCL + 5 mL HNO_3 + 190 mL H_2O) were analyzed by an Olympus GX71 optical microscope(OM) and a Hitachi S−4700 scanning electron microscope(SEM). A Finder 1000 energy dispersive spectrometer (EDS) was used for analyzing the constituents. The melting temperatures of the eutectic phases in different homogenized samples were determined by a Netzsch STA 449C differential scanning calorimetry (DSC). An X′Pert MPD diffractometer (XRD) was used to identify the phases.

All the samples under different homogenization conditions were ground, polished and etched by Barker's etchant for optical microscope observation. The OM images were analyzed using the imaging software. Three samples in the same condition were prepared, and analysis was performed on the three images. The SEM images of the samples after different homogenization treatments were analyzed to investigate the dissolution of the eutectic phases during homogenization. The SEM was operated at 20 kV, and the samples were prepared as the same as that of OM. The DSC experiments were performed with high purity aluminium as a reference. 80−100 mg specimens were prepared using an electro-discharge machine. The heating rate used in the DSC was 10 °C/min. X-ray diffraction (XRD) measurements were performed using a Rigaku D/max-rB X-ray diffractometer with Cu K_α radiation. The scanning from 2θ=10º to 100° was performed to record the XRD pattern.

3 Results and discussion

3.1 As-cast microstructure

Lower and higher magnification SEM images of the microstructure of the as-cast 7X50 aluminum alloy are shown in Fig. 1. The constitutive eutectic phases

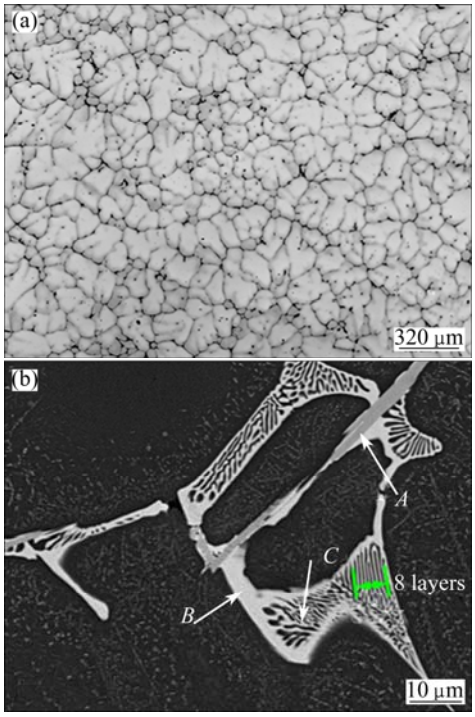

Fig. 1 SEM micrographs of as-cast alloy: (a) Lower magnification; (b) Higher magnification

elongated along the GB can be clearly seen. Different types of eutectic phases are illustrated with arrows in Fig. 1(b). The results of the image analysis indicate that the average spacing of the second dendrite arm is 140 μm, the average width of these eutectic phases is about 2.5 μm and the volume fraction of the eutectic phases is close to 9.2%. The lamellar eutectic structure is shown in Fig. 1(b), and the average width of the lamellas is about 0.8 μm. In order to determine the compositions of different eutectic phases, EDS analysis was performed on the phases with the same morphology. The results show that most of the eutectic phases have the same composition, and the results of EDS analysis of different morphology phases illustrated with arrows in Fig. 1(b) are listed in Table 2. In the as-cast alloy, the gray phase of the fine particles in Al matrix is $MgZn_2$. The deep gray needle-like phase contains Cu and Fe, which is close to Al_7Cu_2Fe phase in composition (spot *A* in Fig. 1(b)), while the gray bone-like phase is $T(Al_2Mg_3Zn_3)$ phase (spot *B* and in Fig. 1(b)), and the lamellar eutectic phase is $S(Al_2CuMg)$ phase (spot *C* in Fig. 1(b)). The gray eutectic phase is also considered to be $T(Al_2Mg_3Zn_3)$ phase with solute of Cu [10−14,24].

Table 2 Chemical compositions of secondary phases in Fig. 1(b)

Phase	*x*(Al)/%	*x*(Zn)/%	*x*(Mg)/%	*x*(Cu)/%	*x*(Fe)/%
A	70.50	−	1.56	18.58	9.36
B	23.66	21.83	32.98	21.53	−
C	61.68	10.87	17.80	9.65	−

3.2 Microstructure of homogenized alloys

Figure 2 shows the TEM images of the alloy after different homogenization treatments. The spherical white dispersoids in Fig. 2 are metastable Al_3Zr. TEM images in Fig. 2 show that a relatively large number and high density of Al_3Zr dispersoids (15−30 nm in diameter) can be observed in the samples homogenized at 400 °C for 10 h and then at 470 °C for 24 h. However, when the samples are homogenized at 470 °C for 24 h, Al_3Zr dispersoids are 20−50 nm in diameter. It was reported that the nucleation rate for the formation of Al_3Zr dispersoids is dependent on the Zr content and temperature [25,26]. The rates of maximum nucleation and growth increase with increasing Zr content and homogenization temperature. Furthermore, it is suggested that at certain Zr content, a high homogenization temperature is required to obtain big Al_3Zr dispersoids and high growth rate. In this work, with 0.10% Zr, the results suggest that homogenization at 400 °C results in both high density and dispersive Al_3Zr phase.

The evolution of eutectic structures during homogenization was investigated. Figure 3 shows the microstructures of specimens homogenized at 470 °C for different time, and at 470 °C for 24 h and then at 482 °C for different time. The EDS analysis results of different morphology phases after different homogenization treatments are listed in Table 3.

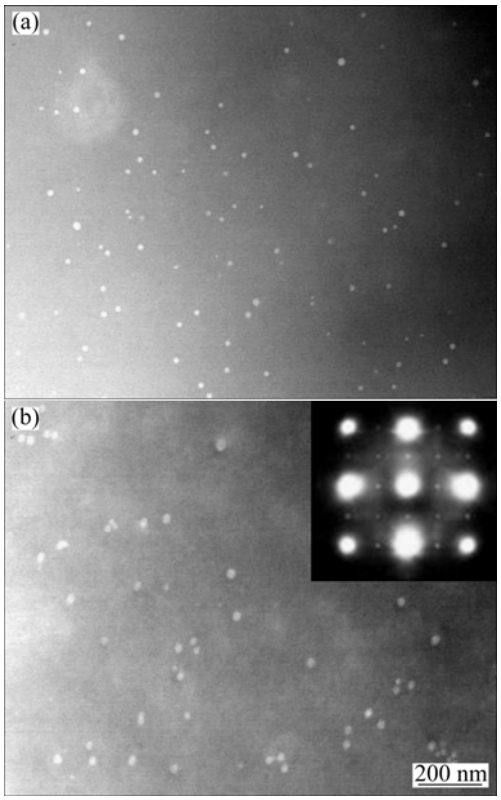

Fig. 2 TEM images showing Al_3Zr dispersoids after being homogenized at 400 °C for 10 h and then at 470 °C for 24 h (a) and at 470 °C for 24 h (b)

Figure 3 shows that the volume fraction of the dendritic-network structure decreases gradually, and the residual phases become smaller and sparser with increasing the homogenization time. The non-equilibrium phases at the grain boundaries also dissolve gradually with increasing the homogenization time. It can be seen from Fig. 3(a) and Table 3 that the area fraction of the eutectic phases decreases to 5.6% and the residual eutectic phases are mainly $T(Al_2Mg_3Zn_3)$, $S(Al_2CuMg)$ and Al_7Cu_2Fe. When the time increases to 24 h at 470 °C, it can be observed from Fig. 3(b) and Table 3 that the $T(Al_2Mg_3Zn_3)$ phase disappears, and the $S(Al_2CuMg)$ phase decreases significantly and the dissolution of Al_7Cu_2Fe is not obvious. It can be seen from Figs. 3(b) and (c) that the $S(Al_2CuMg)$ phase is increasingly dissolved with time going on. The microstructure has no significant change compared with that homogenized at 470 °C for 48 h (Fig. 3(c)) and 96 h (Fig. 3(d)). Figures 3(e) and (f) show the microstructures after homogenization at 470 °C for 24 h and then at

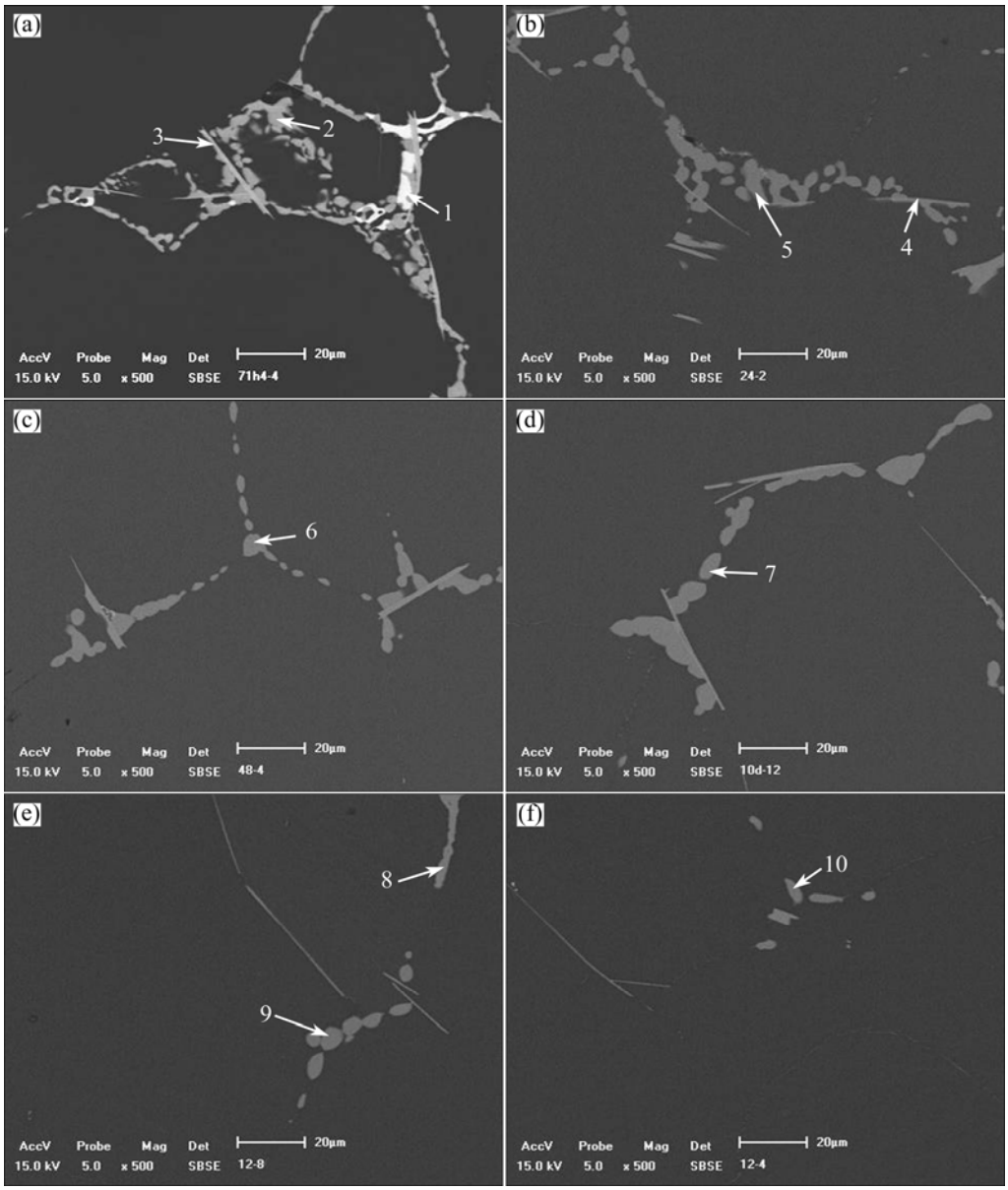

Fig. 3 SEM images of specimens homogenized at different temperatures for different time: (a) 470 °C, 4 h; (b) 470 °C, 24 h; (c) 470 °C, 48 h; (d) 470 °C, 96 h; (e) (470 °C, 24 h) + (482 °C, 12 h); (f) (470 °C, 24 h) + (482 °C, 24 h)

482 °C for 12 h and 24 h, respectively. It can be seen from Fig. 3 and Table 3 that the continuous residual phases along the grain boundaries have turned out to be discontinuous ones and presented to be round or elliptic in shape. When the temperature of the second homogenization stage is 482 °C, the $S(Al_2CuMg)$ phase becomes smaller and almost no change has happened for the Al_7Cu_2Fe [10]. It is also found that, even after homogenization at a higher temperature (482 °C), some of the residual phases do not dissolve completely in the structure. These particles retained are mostly $S(Al_2CuMg)$ and Al_7Cu_2Fe suggested by the EDS analysis in Table 3. It can be concluded that the suitable process of homogenization is 470 °C for 24 h and then at 482 °C for 12 h.

Table 3 Chemical compositions of secondary phases in Fig. 3

Phase	x(Al)/%	x(Mg)/%	x(Zn)/%	x(Cu)/%	x(Fe)/%
1	36.8	29.4	17.4	16.4	−
2	48.8	23.8	3.2	24.2	−
3	85.2	−	−	9.9	4.9
4	75.5	−	−	15.7	8.8
5	47.5	26.7	1.7	24.1	−
6	52.5	24.2	−	23.3	−
7	52.2	23.7	−	24.1	−
8	71.4	−	0.5	18.7	9.4
9	53.6	24.4	−	22.0	
10	54.0	24.1	−	21.9	

3.3 DSC curves of homogenized alloys

The DSC curves of the as-cast ingots and the specimens after homogenization at 470 °C for different time are shown in Fig. 4. Figure 5 shows the enthalpies of peaks 1 (477.8 °C) and 2 (487.5 °C) on different curves of DSC analysis for as-cast alloy, and the specimens homogenized for different time in Fig. 4. For Curve 1 in Fig. 4, a relatively high endothermic peak can be observed when the sample is heated to 477.8 °C and the enthalpy associated with it is 5.935 J/g. This indicates that the constituents will melt at 477.8 °C and the over-burning occurs if the ingots are quickly heated to 477.8 °C after being cast [10,14]. Hence, to avoid over-burning, the conventional homogenization temperature for the semi-continuous casting ingots of the alloy is below 470 °C [14,27]. For Curves 2 and 3 in Fig. 4, the endothermic peak at 477.8 °C becomes smaller after the sample is homogenized at 470 °C for 1 h and 8 h, the enthalpy associated with peak 1 of the sample homogenized at 470 °C for 8 h is only 0.594 J/g. Meanwhile, a new endothermic peak at 487.5 °C (peak 2) is observed, which means that the majority of the constituents melted at 477.8 °C disappear after homogenization at 470 °C for 8 h, and some new constituents melted at 487.5 °C are formed. After homogenization at 470 °C for 8 h, the enthalpy of peak 2 (which is a new and endothermic one) of the sample is the highest. The endothermic peak 1 at 477.8 °C disappears gradually and the enthalpy of the endothermic peak 2 at 487.5 °C becomes smaller with increasing the homogenization time at 470 °C. It may be related to the dissolution of some non-equilibrium phases during homogenization. By prolonging the homogenization treatment time, the constituents melted at 477.8 °C will gradually decrease until they disappear at 470 °C for 24 h, and the amount of those melted at 487.5 °C will become smaller too, as shown on Curves 2−4 of Fig. 4. However, the constituents melted at 487.5 °C still exist during homogenization at 470 °C for 240 h, which means that they cannot be eliminated at this temperature.

Figures 6 and 7 show the DSC curves and the enthalpies of specimens homogenized at 470 °C for 24 h and then at 482 °C for different time, respectively. The endothermic peak and enthalpy at 482 °C for 1 h are the

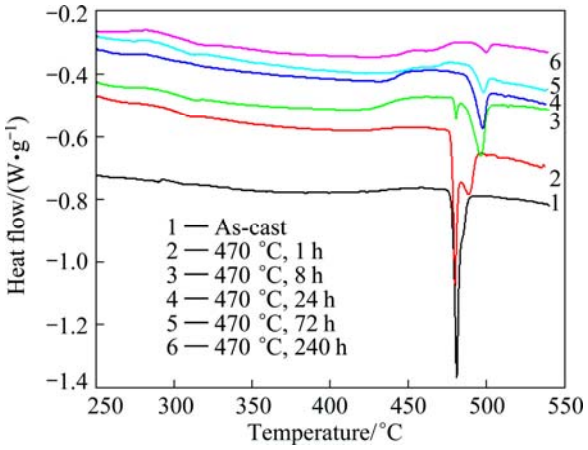

Fig. 4 DSC curves of as-cast ingot and specimens homogenized at 470 °C for different time

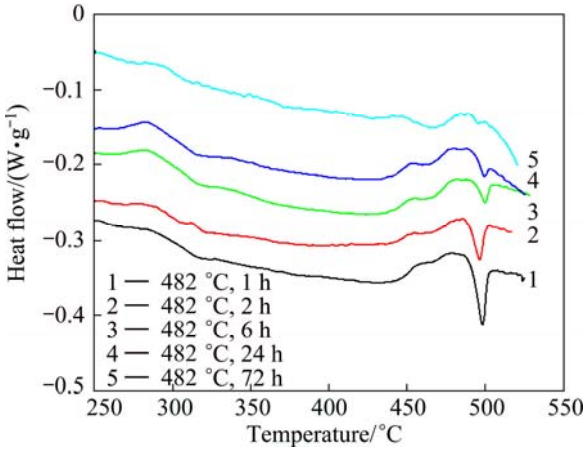

Fig. 6 DSC curves of specimens homogenized at 470 °C for 24 h and then at 482 °C for different time

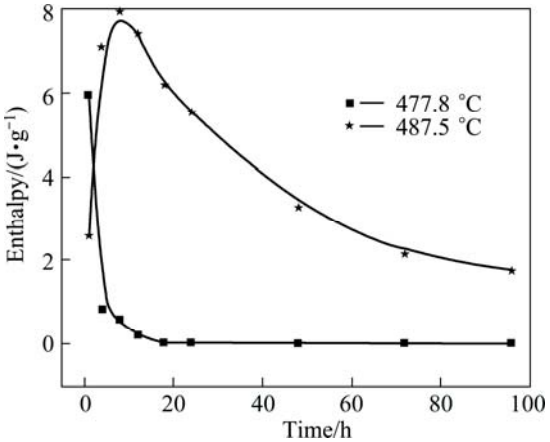

Fig. 5 Enthalpies of endothermic peaks of different DSC curves in Fig. 4

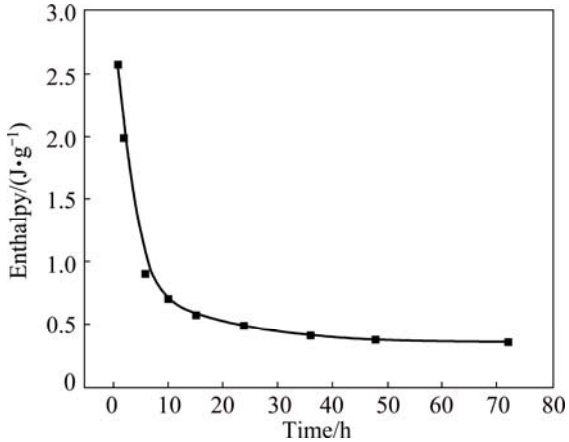

Fig. 7 Enthalpies of endothermic peaks of different DSC curves in Fig. 6

highest. The endothermic peak at 487.5 °C disappears gradually and the enthalpy becomes smaller with increasing the homogenization time at 482 °C, as shown on the curves 1−4 in Fig. 6. The majority of the constituents melted at 487.5 °C disappear after homogenization at 482 °C for 24 h, and the enthalpy associated with the peak at 487.5 °C of the sample homogenized is only 0.476 J/g, which means that they are almost eliminated at 482 °C for 24 h.

3.4 XRD patterns of homogenized alloys

It is possible to identify these phases in the as-cast and as-homogenized materials by XRD analysis. The XRD patterns are shown in Fig. 8. In the as-cast alloy, XRD peaks arise from the (Al), $MgZn_2$, Al_2CuMg and Al_3Zr phases. The gray phase of the fine particles in Al matrix is $MgZn_2$ as shown in Fig. 1(b). In the as-homogenized alloy, XRD peaks are also related to the (Al), $MgZn_2$, Al_2CuMg and Al_3Zr phases. The XRD peak of Al_2CuMg in the alloy homogenized at 470 °C for 48 h is smaller. The XRD peaks of Al_2CuMg and $MgZn_2$ are the smallest in the alloy homogenized at 470 °C for 24 h and then at 482 °C for 24 h. Small amounts of Fe-rich phases, Al_2Cu and Mg_2Si may exist. It can be concluded that the $MgZn_2$, Al_2CuMg and Al_3Zr exist in the as-cast and as-homogenized alloys, but the T ($Al_2Mg_3Zn_3$) phase cannot be observed, which means that the gray eutectic phases are considered to be associated with S (Al_2CuMg) phase and $MgZn_2$ phase [10,28].

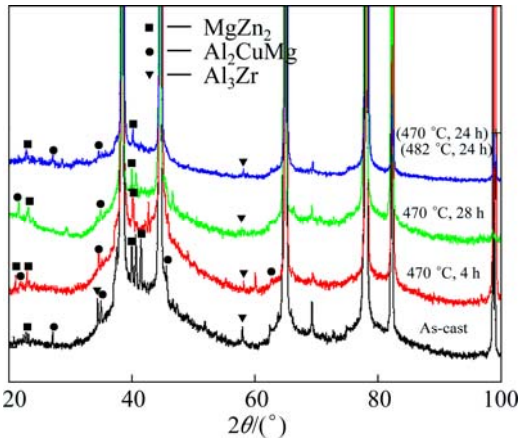

Fig. 8 XRD patterns of as-cast alloy and specimens after homogenization treatment

3.5 Microstructure of plate

Figure 9 shows optical micrographs of plate subjected to hot rolling, solution and aging treatment after pre-homogenization and conventional homogenization treatment. The unrecrystallized material is readily identified as the dark regions. It is apparent that the recrystallized fraction is substantially less in the material with pre-homogenization treatment. In the material with

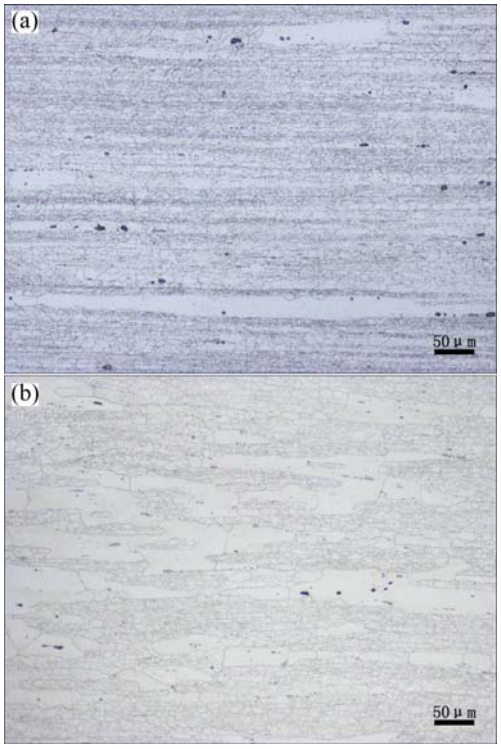

Fig. 9 Optical micrographs of heat-treated 7X50 alloy: (a) Pre-homogenization; (b) Conventional homogenization

conventional homogenization treatment, continuous wide recrystallized bands form and the measured recrystallized fraction is 43%. In contrast, in the material subjected to a pre-homogenization treatment, the recrystallized regions are not interconnected and the measured recrystallized fraction is 18%. This is mainly because of the Al_3Zr particles coherent to subgrain boundary and grain boundary migration hindrance, thus inhibiting recrystallization and growth. The pre-homogenization procedure involves using lower temperature hold to encourage Al_3Zr dispersoid nucleation prior to conventional homogenization. The improved dispersoid distribution is more effective in suppressing recrystallization during subsequent processing, approximately halving the recrystallized fraction from that in the material subjected to conventional homogenization.

3.6 Mechanical properties of plate

Table 4 shows the mechanical properties of the plate subjected to hot rolling, solution and aging treatment after different homogenization treatment. It is apparent that the strength and fracture toughness of the material with pre-homogenization treatment are higher. The strength and fracture toughness of the material with pre-homogenization treatment are about respectively 15 MPa and 3.3 $MPa{\cdot}m^{1/2}$ higher than those of the material with a conventional homogenization treatment. The pre-homogenization procedure encourages Al_3Zr

dispersoid nucleation and the Al_3Zr particle efficiently inhibits the recrystallization and growth. The fraction of low intensive recrystallization reduces and the substructure strengthening improves. The subgrain boundary can efficiently promote the nucleation and precipitation of the second phase particle, and therefore improve the strength of material.

Table 4 Mechanical properties of plate processed by different homogenization processes

Homogenization process	Tensile strength/ MPa	Yield strength/ MPa	Elongation/ %	Fracture toughness (L−T)/ (MPa·m$^{1/2}$)
Pre-homogenization	599	558	11.7	27.75
Conventional homogenization	584	545	10.5	24.45

4 Conclusions

1) Severe dendritic segregation exists in 7X50 alloy ingot, and the main phases are S(Al_2CuMg), T($Al_2Mg_3Zn_3$), $MgZn_2$, with small amounts of Al_7Cu_2Fe and Al_3Zr phases. A relatively high endothermic peak at 477.8 °C in as-cast 7X50 alloy can be observed and the enthalpy is 5.935 J/g.

2) The volume fraction of the dendritic-network structure decreases gradually and the residual phases become smaller and sparser by prolonging the homogenization time. The T($Al_2Mg_3Zn_3$) phase disappears, minimal S(Al_2CuMg) phase remains, and almost no change has happened for the Al_7Cu_2Fe homogenized at 470 °C for 24 h and then at 482 °C for 12 h.

3) The DSC curve of the as-cast alloy has a relatively strong endothermic peak at 477.8 °C. A new endothermic peak at 487.5 °C appears for the samples homogenized at 470 °C and the endothermic peak at 477.8 °C gradually disappears. The majority of the constituents melted at 487.5 °C disappear after homogenization at 482 °C for 24 h.

4) The recrystallized fraction is substantially less in the material with pre-homogenization treatment. The strength and fracture toughness of the material with pre-homogenization treatment are about 15 MPa and 3.3 MPa·m$^{1/2}$ higher than those of the material with conventional homogenization treatment.

Acknowledgements

The authors are grateful to the Northeast Light Alloy Co., Ltd., for production and provision of the materials. The authors also appreciate LI Zhi-hui and ZHANG Yong-an of Beijing General Research Institute of Nonferrous Metals, and YIN Zhi-min and JIANG Feng of Central South University for valuable discussions and recommendations.

References

[1] ROBSON J D. Microstructural evolution in aluminium alloy 7050 during processing [J]. Materials Science and Engineering A, 2004, 382(1−2): 112−121.

[2] MARTIN J W. Precipitation hardening [M]. Oxford: Butterworth-Heinemann, 1998: 79−111.

[3] LALPOOR M, ESKIN D G., RUVALCABA D, FJAER H G., TEN CATE A, ONTIJT N, KATGERMAN L. Cold cracking in DC-cast high strength aluminum alloy ingots: An intrinsic problem intensified by casting process parameters [J]. Materials Science and Engineering A, 2011, 528(6): 2831−2842.

[4] ROBSON J D, PRANGNELL P B. Dispersoid precipitation and process modelling in zirconium containing commercial aluminium alloys [J]. Acta Materialia, 2001, 49(4): 599−613.

[5] ROBINSON J S. Influence of retrogression and reaging on fracture toughness of 7010 aluminium alloy [J]. Materials Science and Technology, 2003, 19(12): 1697−1704.

[6] LIU H S, QIAO X, CHEN Z H, JIANG R P, LI X Q. Effect of ultrasonic vibration during casting on microstructure and properties of 7050 aluminum alloy [J]. Journal of Materials Science, 2011, 86(11): 3923−3927.

[7] BELIN F E, FOURNEE V, MIZUTANI U, TAKEUCHI T, MULLER H. Investigation of Al and Mg occupied densities of states of Al−Mg−Zn alloys [J]. Materials Science and Engineering A, 2000, 294−296(12): 516−518.

[8] XU D K, ROMETSCH P A, BIRBILIS N. Improved solution treatment for an as-rolled Al−Zn−Mg−Cu alloy. Part I: Characterisation of constituent particles and overheating [J]. Materials Science and Engineering A, 2012, 534(1): 234−243.

[9] LI X M, STARINK M J. The effect of compositional variations on characteristics of coarse intermetallic particles in overaged 7000 aluminium alloys [J]. Materials Science and Technology, 2001, 17(11): 1324−1328.

[10] FAN X G, JANG D M, MENG Q C, LI Z. The microstructural evolution of an Al−Zn−Mg−Cu alloy during homogenization [J]. Materials Letters, 2006, 60(12): 1475−1479.

[11] LÜ X Y, GUO E J, LI Z H, WANG G J. Research on microstructure in as-cast 7A55 aluminum alloy and its evolution during homogenization [J]. Rare Metals, 2011, 30(6): 664−668.

[12] EIVANI A R, AHMED H, ZHOU J, DUSZCZYK J. Evolution of grain boundary phases during the homogenization of AA7020 aluminum alloy [J]. Metallurgical and Materials Transactions A, 2009, 40(3): 717−728.

[13] HE L Z, LI X H, ZHU P, CAO Y H, GUO Y P, CUI J Z. Effects of high magnetic field on the evolutions of constituent phases in 7085 aluminum alloy during homogenization [J]. Materials Characterization, 2012, 71(9): 19−23.

[14] DENG Y, YIN Z M, CONG F G. Intermetallic phase evolution of 7050 aluminum alloy during homogenization [J]. Intermetallics, 2012, 26(7): 114−121.

[15] XIE F Y, YAN X Y, DING L, ZHANG F, CHEN S L, HU M G, CHENG Y A. A study of microstructure and microsegregation of aluminum 7050 alloy [J]. Materials Science and Engineering A, 2003, 355(1−2): 144−153.

[16] ROKHLIN L L, DOBATKINA T V, BOCHVAR N R, LYSOVA E V. Investigation of phase equilibria in alloys of the Al−Zn−Mg−Cu−Zr−Sc system [J]. Journal of Alloys and Compounds, 2004, 367(1−2): 10−16.

[17] LI X M, STARINK M J. Identification and analysis of intermetallic phases in overaged Zr-containing and Cr-containing Al−Zn−Mg−Cu alloys [J]. Journal of Alloys and Compounds, 2011, 509(2): 471−476.
[18] LI Y X, LI P, ZHAO G, LIU X T, CUI J Z. The constituents in Al−10Zn−2.5Mg−2.5Cu aluminum alloy [J]. Materials Science and Engineering A, 2005, 397(1−2): 204−208.
[19] DONG J, CUI J Z, ZENG X Q, DING W J. Effect of low-frequency electromagnetic field on microstructures and macrosegregation of Φ270 mm DC ingots of an Al−Zn−Mg−Cu−Zr alloy [J]. Materials Letters, 2005, 59(12): 1502−1506.
[20] MONDAL C, MUKHOPADHYAY A K. On the nature of $T(Al_2Mg_3Zn_3)$ and $S(Al_2CuMg)$ phases present in as-cast and annealed 7055 aluminum alloy [J]. Materials Science and Engineering A, 2005, 391(1−2): 367−376.
[21] ZHAO Z H, CUI J Z, DONG J, ZHANG B J. Effect of low-frequency magnetic field on microstructures and macrosegregation of horizontal direct chill casting 7075 aluminum alloy [J]. Journal of Materials Processing Technology, 2007, 182(1−3): 185−190.
[22] RANGANATHA R, KUMAR V A, NNANDI V S, NURALIDHARA B K. Multi-stage heat treatment of aluminum alloy AA7049 [J]. Transactions of Nonferrous Metals Society of China, 2013, 23(6): 1570−1575.
[23] LIM S T, LEE Y Y, EUN I S. Microstructural evolution during ingot preheat in 7xxx aluminium alloys for thick semiproduct applications [J]. Materials Science Forum, 2006, 519−521(7): 549−554.
[24] CELENTANO D J. A thermomechanical model with microstructure evolution for aluminium alloy casting processes [J]. International Journal of Plasticity, 2002, 18(10): 1291−1335.
[25] ENGLER O. Nucleation and growth during recrystallization of aluminium alloys investigated by local texture analysis [J]. Materals Science and Technology, 1996, 12(10): 859−872.
[26] ROBSON J D. Optimizing the homogenization of zirconium containing commercial aluminium alloys using a novel process model [J]. Materials Science and Engineering A, 2002, 338(1−2): 219−229.
[27] LI X M, STARINK M J. DSC study on phase transitions and their correlation with properties of overaged Al−Zn−Mg−Cu alloys [J]. Journal of Materials Engineering and Performance, 2012, 21(6): 977−984.
[28] WU L M, WANG W H, HSU Y F, TRONG S. Effects of homogenization treatment on recrystallization behavior and dispersoid distribution in an Al−Zn−Mg−Sc−Zr alloy [J]. Journal of Alloys and Compounds, 2008, 456(1−2): 163−169.

均匀化处理对 DC 铸造 7X50 铝合金显微组织和力学性能的影响

丛福官[1,2]，赵 刚[1]，姜 锋[3]，田 昵[1]，李瑞峰[1]

1. 东北大学 材料各向异性与织构教育部重点实验室，沈阳 110004；
2. 东北轻合金有限责任公司，哈尔滨 150060；
3. 中南大学 材料科学与工程学院，长沙 410083

摘 要：采用 SEM、TEM、EDS、DSC、XRD 和拉伸实验研究铸态 7X50 合金及其均匀化处理过程的组织演变。结果表明，铸态 7X50 合金相组成主要有 $S(Al_2CuMg)$、$T(Al_2Mg_3Zn_3)$、$MgZn_2$ 和少量的 Al_7Cu_2Fe 和 Al_3Zr 相。均匀化处理过程中枝晶网和残留相逐渐减少，经(470 °C，24 h)+(482 °C，12 h)均匀化处理时，T 相消失，S 相有微量残留，Al_7Cu_2Fe 相几乎没有变化。铸态合金的 DSC 曲线中在 477.8 °C 处有一较强吸热峰，经 470 °C、1 h 均匀化后合金的 DSC 曲线在 487.5 °C 处出现一个新的吸热峰，而经 482 °C、24 h 均匀化处理后合金在 487.5 °C 处的吸热峰基本消失。在 XRD 谱中未出现 $T(Al_2Mg_3Zn_3)$相，这和 T 相与 $S(Al_2CuMg)$及 $MgZn_2$ 相相关的结论相吻合。预均匀化处理制备的板材中再结晶晶粒分数明显降低，抗拉强度和断裂韧性相对常规均匀化处理制备的板材分别提高约 15 MPa 和 3.3 $MPa\cdot m^{1/2}$。

关键词：7X50 铝合金；组织演变；均匀化处理；残余相；再结晶

(Edited by Wei-ping CHEN)